Progress In Electromagnetics Research C, Vol. 41, 81–95, 2013

A COMPACT DUAL-BAND BAND-PASS FILTER WITH WIDE STOP-BAND USING TWO RESONATORS COMBINED BY VIA-HOLE

Fang Xu[1], Zongjie Wang[1], Mi Xiao[1, *], Jizong Duan[1], Jiayang Cui[1], Zhe Zhu[1], Mu Ju[2], and Yang Liu[1]

[1]School of Electronic Information Engineering, Tianjin University, Tianjin 300072, China

[2]Southeast University, Nanjing 211100, China

Abstract—A compact dual-band band-pass filter is proposed in this paper. The central frequencies of the passbands are around 2.46 GHz and 5.86 GHz. There are two resonators located at the top side layer and the bottom side (the CPW) layer, respectively. Dual-resonance operation usually needs two resonators on the same layer to generate two passbands simultaneously. However, in this paper the size can be reduced efficiently by connecting resonators at two layers through via-holes to implement dual-band performance. Furthermore, the stop-band for this novel filter with T slot-line, L-line and rectangular micro-strips can be extended to 30 GHz. To verify the feasibility of the design above, a dual-band band-pass filter has been implemented on a Rogers RT5880 substrate (thickness is 0.508 mm). This filter with passbands operated at 2.46 GHz and 5.86 GHz can finely meet the IEEE 802.11n wireless local area network (WLAN) bands requirements.

1. INTRODUCTION

With the ever-increasing demand for application flexibility, the designs of many passive circuits, such as the bandpass filters, are facing new design challenges including compact size, wide bandwidth and multi-band operations. More and more wireless systems are leaning towards dual-band and multi-band operation. For example, high-speed wireless local area networks (WLANs) for IEEE 802.11n operating simultaneously at both 2.4 GHz–2.48 GHz and 5.8 GHz–5.88 GHz bands have been developed. To accommodate these dual-band communication systems, devices such as dual-band antennas,

Received 12 May 2013, Accepted 6 June 2013, Scheduled 17 June 2013

* Corresponding author: Mi Xiao (xiaomi@tju.edu.cn).

dual-band baluns and dual-band filters with high performance are required. Dual-band band-pass filters are the important components for the communication systems. The methods have been already proposed to implement the dual-band band-pass filter [1–14]. The stepped impedance resonators (SIRs), E-shaped microstrip SIRs and GSIRS are also employed to achieve dual-band performance utilizing the fundamental frequency and second harmonic passband [1, 2, 10, 13] but it is not convenient to meet a specific bandwidth requirement. Besides, two independent resonators are combined [3, 4]. Recently, dual-feeding structures [5], the parallel coupled microstrip line [6], dual-plane defected structures [7], multi-stub-loaded resonators [8], the circuit consisting two two-port networks in shunt connection [9], square loop resonators [11], short-ended dual-mode resonators [12] and coupled three-line resonators [14] are all introduced in dual-band performance design. However, these methods are at the sacrifice of relative large size and the stop-band of those filters is not wide enough. In this paper, a novel compact dual-band band-pass filter with the stop-band up to 30 GHz is implemented and the dual-band pass-bands are located at 2.43 GHz–2.52 GHz and 5.83 GHz–5.92 GHz. The well performance above is realized in a compact size as small as 24 mm ∗ 14.7 mm, through connecting two resonators at different layers by via-holes.

2. THE FILTER DESIGN

A original band-pass filter and the resonator of the filter are shown in Fig. 1(a) for the readers. A pass-band ranging from 2.40 GHz to

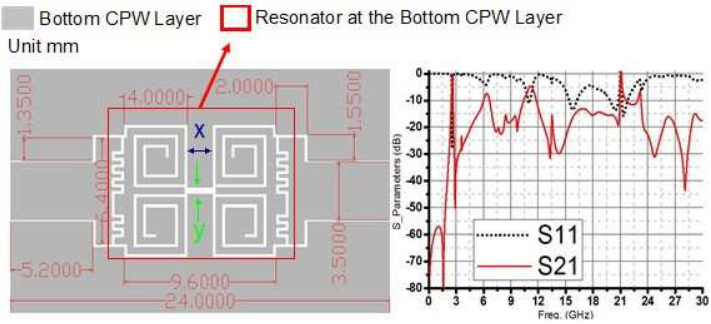

Figure 1. The original band-pass filter. (a) Filter structure. (b) The simulated frequency response for the filter.

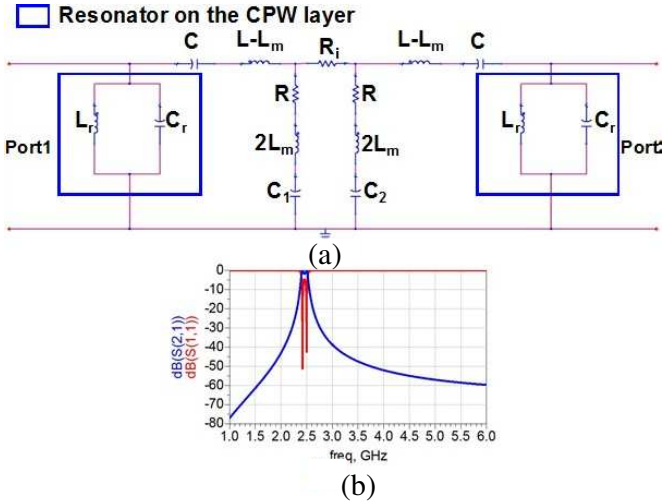

Figure 2. The simplified circuit model for the original band-pass filter. (a) The equivalent circuit model. (b) The simulated frequency response in ADS ($C_r = 63\,\text{pF}$, $L_r = 63\,\text{pH}$, $L - L_m = 19.2474\,\text{pH}$, $R = 0.5\,\text{ohm}$, $2L_m = 1.979\,\text{pH}$, $C = 6\,\text{pF}$, $C_1 = 1.58\,\text{pF}$, $C_2 = 1\,\text{pF}$, $R_i = 1\,\text{ohm}$).

2.48 GHz has been created. Furthermore, the equivalent simplified circuit model is presented in Fig. 2.

The R_i in Fig. 2(a) stands for the connecting resistance between the left side and right side of the resonator on the CPW layer. However, the resistance loss for the resonator (CPW layer) is small enough so that the R_i in the transmission function can be ignored. Besides, the coupling influence equivalent network between two side of the resonator is represented by C, $L - L_m$, R, C_m, C_1 and C_2. Those components are combined to illustrate the mixed coupling theory to the two sides of this resonator in Fig. 1. Detailed explanation for the mixed coupling theory has been proposed in [16]. In order to illustrate the equivalent circuit model in detail and obtain the transmission function (S_{21}) of the whole circuit, the variables A, B and C are assumed as:

$$A = \frac{1}{\left(\frac{1}{R + 2j\omega L_m + \frac{1}{j\omega C_1}}\right) + \left(\frac{1}{R + 2j\omega L_m + \frac{1}{j\omega C_2}}\right) + \left(\frac{1}{j\omega(L - L_m) + \frac{1}{j\omega C} + \frac{1}{\frac{1}{j\omega L_r} + j\omega C_r + \frac{1}{Z_0}}}\right)}; \quad (1)$$

$$B = \frac{1}{\left(\frac{1}{j\omega L_r} + j\omega C_r\right)} + \frac{1}{j\omega C} + j\omega(L - L_m) + A; \tag{2}$$

$$D = \frac{1}{\frac{1}{j\omega L_r} + j\omega C_r + \left(\frac{1}{\frac{1}{j\omega C} + j\omega(L-L_m)+A}\right)}; \tag{3}$$

Finally, the S_{21} expression for the circuit model is as follows:

$$S_{21} = \left(\frac{2}{\frac{1}{j\omega L_r} + j\omega C_r}\right) \cdot \frac{\left(\frac{1}{\left(\frac{1}{R+2j\omega L_m+\frac{1}{j\omega C_1}}\right)+\left(\frac{1}{R+2j\omega L_m+\frac{1}{j\omega C_2}}\right)}\right)}{\left(\frac{1}{\left(\frac{1}{R+2j\omega L_m+\frac{1}{j\omega C_1}}\right)+\left(\frac{1}{R+2j\omega L_m+\frac{1}{j\omega C_2}}\right)} + j\omega(L-L_m) + \frac{1}{j\omega C} + \left(\frac{1}{\frac{1}{j\omega L_r} + j\omega C_r + \frac{1}{Z_0}}\right)\right)}{B(Z_0 + D)}; \tag{4}$$

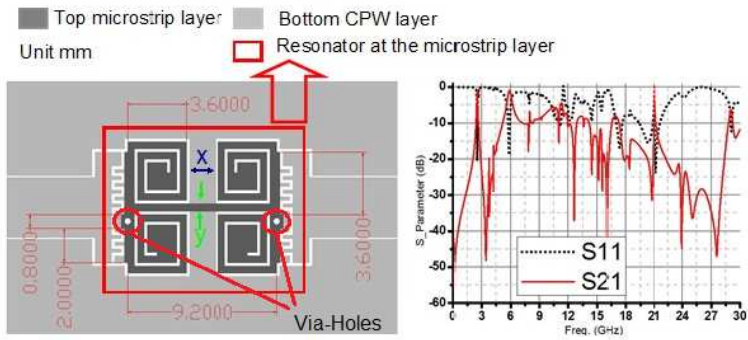

(a) (b)

Figure 3. The dual-band bandpass filter with two resonators connecting by via-holes. (a) The filter structure. (b) The simulated frequency response.

Then, a filter with two resonators connecting by via-holes is proposed based on the filter in Fig. 1(a). The resonator on the second layer (micro-strip layer) is introduced to generate the second passband ranging from 5.8 GHz to 5.88 GHz shown in Fig. 3. According to the simulated frequency response for the filter in Figs. 1(b) and 2(b), we can know that a dual-band performance filter in Fig. 3(a) using two resonators has been realized. The two pass-bands are from 2.4 GHz to 2.48 GHz and 5.8 GHz to 5.88 GHz, respectively. The equivalent simplified circuit model is also given in Fig. 6. The two resonators may be represented by the parallel L-C resonant loop as same as the Fig. 2 and the via-holes can be thought as a L-C series circuit. Furthermore, the simulated results (computed results) based on the simplified models in Figs. 2 and 4 show the similarity with simulated results in Figs. 1 and 3. In order to study the micro-strip resonator we added on the top layer in detail, the filter with only one resonator on

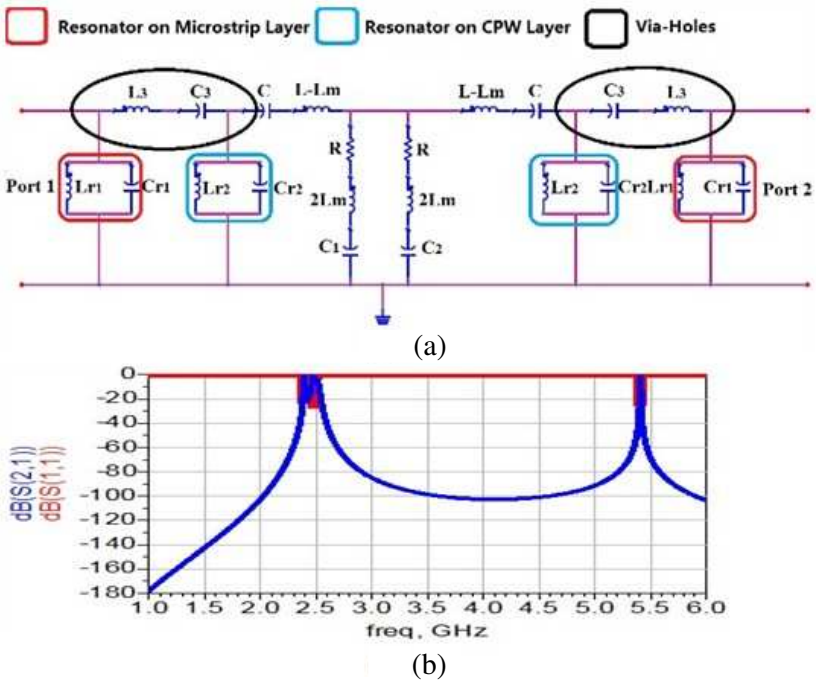

Figure 4. The simplified circuit model for the dual-band band-pass filter. (a) The equivalent circuit model. (b) The simulated frequency response in ADS ($C_{r1} = 63$ pF, $L_{r1} = 63$ pH, $C_{r2} = 63$ pF, $L_{r2} = 63$ pH, $L - L_m = 19.2474$ pH, $R = 0.5$ ohm, $2L_m = 1.979$ pH, $C = 6$ pF, $C_1 = 1.58$ pF, $C_2 = 1$ pF, $L_3 = 0.9$ nH, $C_3 = 1$ pF, $R_i = 1$ ohm).

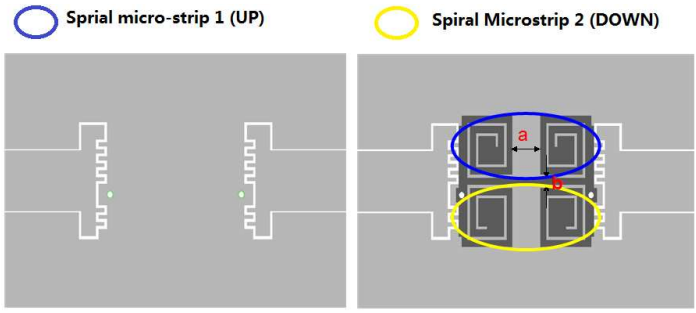

Figure 5. The filter with only micro-strip resonator on the top layer. (a) The bottom layer. (b) The top layer.

the top layer(micro-strip layer) is shown in Fig. 4. And the simulated results of this schematic is presented in and Fig. 6. It can be inferred from Fig. 5 that the micro-strip structure can create one resonate point to form a pass-band. Moreover, the pass-band can be adjusted by changing the distance a, b and the total length of the micro-strip resonator. All of those parameters is marked in Fig. 4. According to Fig. 5, we can conclude that the distance between left and right parts a and the total length of the up micro-strip will significantly affect the resonate frequency of the resonator. However, the width of connecting lines b and the total length of down microstrip contributes little to the resonate frequency movement. So through the carefully adjustment and the coupling effect of two resonators, the extra-passband generated by the microstrip resonator can be located at about 5.8 GHz frequency band to form a dualband filter.

To calculate the expression of the transmission function, the variables M, N, E, F, G, H, I, J, K, Q, W are assumed as follows:

$$M = \frac{1}{\frac{1}{j\omega L_{r1}} + j\omega C_{r1} + \frac{1}{Z_0}}; \tag{5}$$

$$N = \frac{1}{\frac{1}{j\omega C_3} + j\omega L_3 + M}; \tag{6}$$

$$E = \frac{1}{\frac{1}{j\omega L_{r2}} + j\omega C_{r2} + N}; \tag{7}$$

$$F = \frac{1}{j\omega(L - L_m) + \frac{1}{j\omega C} + E}; \tag{8}$$

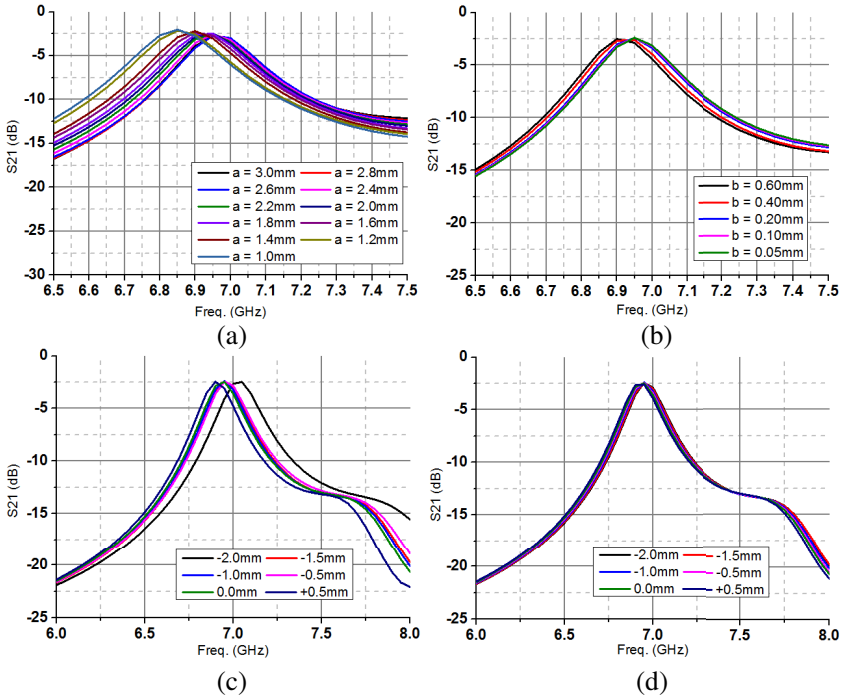

Figure 6. The frequency responses of filter in Fig. 5 for the pass-band for different a, b and length of micro-strips. (a) The frequency responses for different a. (b) The frequency responses for different b. (c) The frequency responses for different total lengths of the spiral micro-strips 1(UP) in Fig. 5. (d) The frequency responses for different total lengths of the spiral micro-strips 2(DOWN) in Fig. 5.

$$G = \frac{1}{\left(\frac{1}{R+2j\omega L_m+\frac{1}{j\omega C_1}}\right)+\left(\frac{1}{R+2j\omega L_m+\frac{1}{j\omega C_2}}\right)+F}; \tag{9}$$

$$H = \frac{1}{\frac{1}{j\omega C}+j\omega(L-L_m)+G}; \tag{10}$$

$$I = \frac{1}{\frac{1}{j\omega L_{r2}}+j\omega C_{r2}+H}; \tag{11}$$

$$J = \frac{1}{\frac{1}{j\omega C_3}+j\omega L_3+I}; \tag{12}$$

$$K = \frac{\left(\frac{1}{\left(\frac{1}{R+2j\omega L_m+\frac{1}{j\omega C_1}}\right)+\left(\frac{1}{R+2j\omega L_m+\frac{1}{j\omega C_2}}\right)}\right)}{\left(\frac{1}{\left(\frac{1}{R+2j\omega L_m+\frac{1}{j\omega C_1}}\right)+\left(\frac{1}{R+2j\omega L_m+\frac{1}{j\omega C_2}}\right)}\right)+\frac{1}{F}}; \quad (13)$$

$$Q = \frac{\left(\frac{1}{\frac{1}{j\omega L_{r1}}+j\omega C_{r1}}\right)}{\frac{1}{N}+\left(\frac{1}{\frac{1}{j\omega L_{r1}}+j\omega C_{r1}}\right)}; \quad (14)$$

$$W = \frac{\left(\frac{1}{\frac{1}{j\omega L_{r2}}+j\omega C_{r2}}\right)}{\frac{1}{H}+\left(\frac{1}{\frac{1}{j\omega L_{r2}}+j\omega C_{r2}}\right)}; \quad (15)$$

So the S_{21} expression for the dualband-filter simplified circuit model is as follows:

$$S_{21} = \frac{2\cdot\left(\frac{\left(\frac{1}{\frac{1}{j\omega L_{r1}}+j\omega C_{r1}}\right)}{J+\left(\frac{1}{\frac{1}{j\omega L_{r1}}+j\omega C_{r1}}\right)}\right)\cdot\left(\frac{I}{j\omega L_3+\frac{1}{j\omega C_3}+I}\right)\cdot W \cdot\left(\frac{G}{\frac{1}{j\omega C}+j\omega(L-L_m)+G}\right)\cdot K\cdot Q\cdot\left(\frac{E}{j\omega(L-L_m)+\frac{1}{j\omega C}+E}\right)\cdot\left(\frac{M}{j\omega C_3+\frac{1}{j\omega C_3}+M}\right)}{\left(\frac{1}{\frac{1}{j\omega L_{r1}}+j\omega C_{r1}+J}\right)+Z_0}; \quad (16)$$

According to Figs. 1 and 3, it can be inferred that the resonator shown at the top side and the other resonator at the bottom side has generated two passbands respectively so that the dual-band pass-band is achieved by combining the two resonators. Furthermore, this design method that two individual resonators on two layers are connected through the via-hole can reduce the size of the dual-band band-pass filter. Besides, the two passbands are controllable through changing the distance x and y in Fig. 3(a) and Fig. 1(a). The simulated results shown in Fig. 8 demonstrate that when the distance y increases the passbands

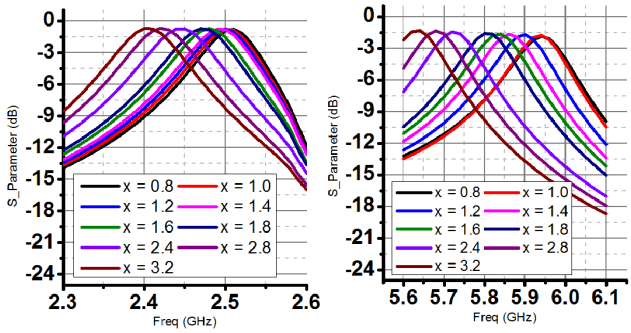

Figure 7. The relationship between the passband position and distances x in Figs. 1 and 3. (a) The first passband frequency responses for different distances x. (b) The second passband frequency responses for different distances x.

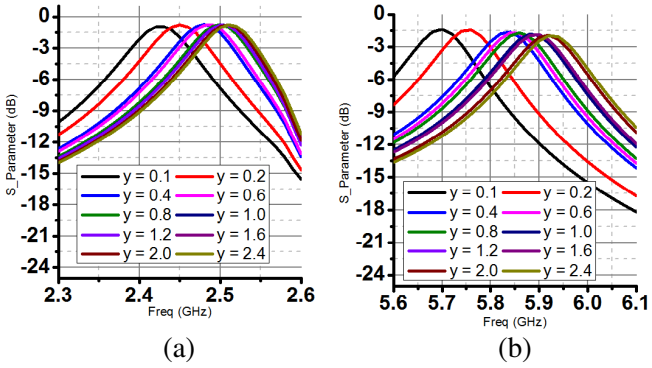

Figure 8. The relationship between the passband position and distances y in Figs. 1 and 3. (a) The first passband frequency responses for different distances y. (b) The second passband frequency responses for different distances y.

at 2.4 GHz and 5.83 GHz will move to higher frequency band while the trend shown in Fig. 7 is opposite for the distance x. As for the location of the via-holes, according to [15], the position of via-holes should be located between the CPW resonator and the meandering lines, so the the available room for via-holes is narrow in this structure. Thus, the difference in size and position of the via-holes will bring little effect to the coupling.

Although the dual-band performance has been achieved, the

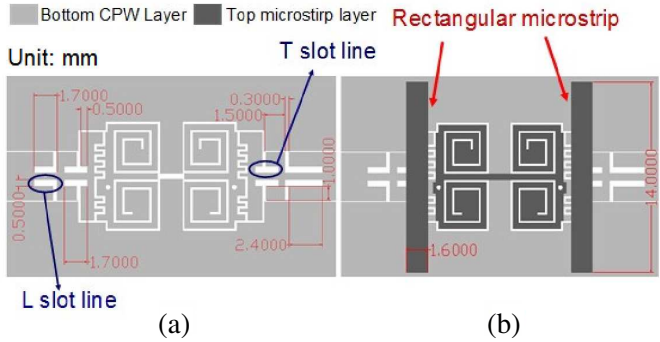

Figure 9. The novel dual-band bandpass filter proposed in this paper. (a) The bottom layer. (b) The top layer.

higher harmonics (spurious responses) appear around high frequencies shown in Fig. 3(b). Those spurious passbands will affect the high frequency performance of the filter. It means that in the high frequency band, more unwanted signals will pass the filter and create bad influence for the whole wireless communication systems. There are several ways to suppress the spurious response including air-bridges, open-stubs and slot-lines.

For this microstrip and CPW coupling structure, the rectangular micro-strips, L slot-lines and T slot-lines shown in Fig. 9 are introduced to suppress the spurious responses. Generally speaking, the rectangular micro-strips can generate transmission zero around 13 GHz. T and L slot-lines can create transmission zeros at about 18 GHz and 25 GHz. The introduction of those structures will significantly improve the high frequency performance of the filter and bring a wide-stopband.

As shown in Fig. 10, the spurious response around $9f_0$ is suppressed after the L slot lines added. Then, in order to reduce the spurious response around $11f_0$, the T slot lines are also introduced. Finally, the harmonic response around $7f_0$ has disappeared after adding the rectangular microstrips. So the stop-band performance is improved significantly. The equivalent circuit models of those higher harmonic suppression structures have already been discussed in [16]. Moreover, the measured frequency response in Fig. 12 demonstrated that the spurious passbands under 30 GHz can be all reduced.

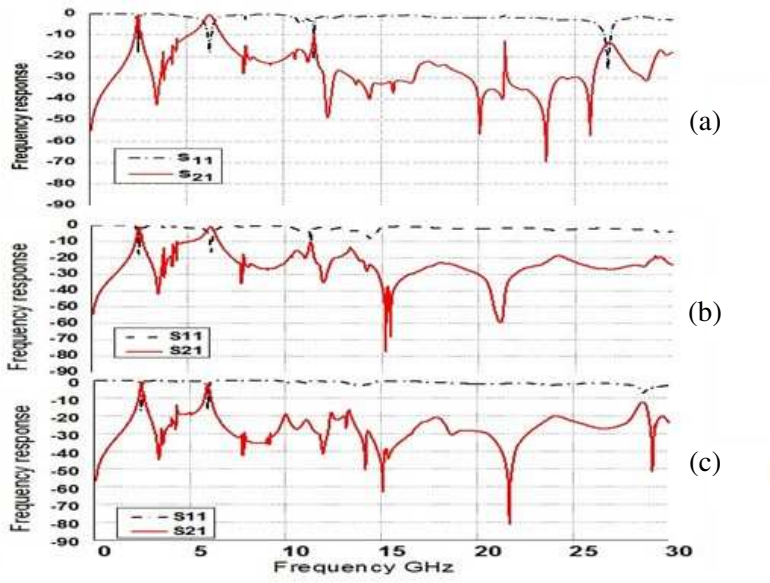

Figure 10. (a) The simulated frequency response for the filter only with L-slot lines (add the L slot-lines to the filter in Fig. 3). (b) The simulated frequency response for the filter with L-slot lines and T-slot lines (add the L slot-lines and T slot-lines to the filter in Fig. 3). (c) The simulated frequency response for the filter proposed in Fig. 7 (with T, L-Slot lines and rectangular microstrip).

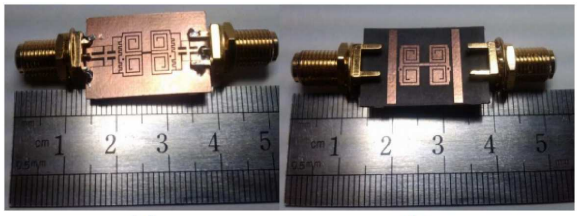

(a) (b)

Figure 11. The fabricated prototype filter. (a) The bottom layer. (b) The top layer.

3. THE MEASURED RESULTS ANALYSIS

To verify the function of the proposed filter, a slot line filter has been fabricated on a Rogers RT5880 substrate ($\varepsilon_r = 2.2$, thickness

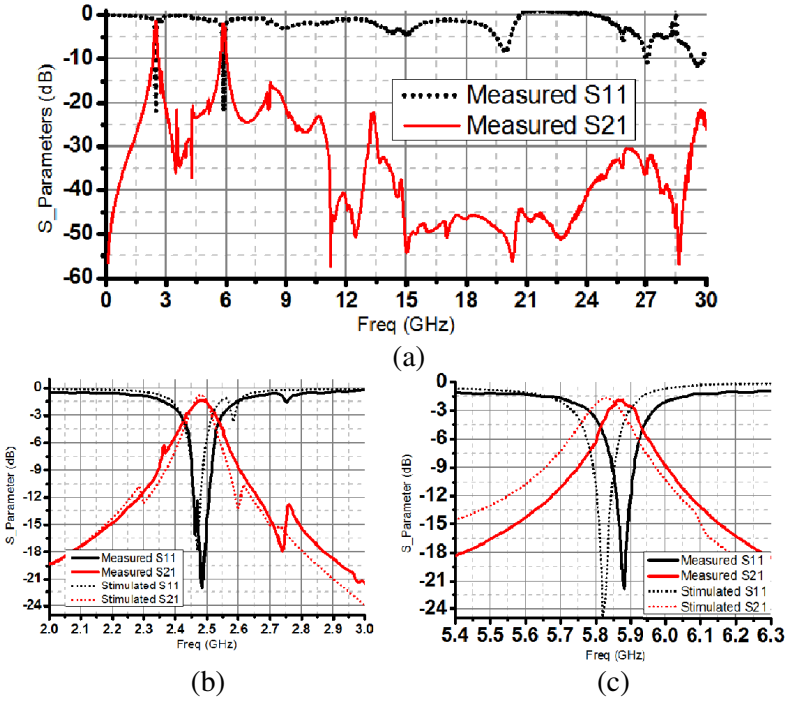

Figure 12. The measured frequency response of the filter. (a) Whole band. (b) Measured and stimulated frequency response at 2.4 GHz passband. (c) Measured and stimulated frequency response at 5.8 GHz passband.

$h = 0.508$ mm), as shown in Fig. 11. The I/O ports' resistance is 50 ohm and the measured results show that the implemented dual-band band-pass filter has two passbands located at 2.43 GHz–2.52 GHz and 5.83 GHz–5.92 GHz with the typical insertion loss of 21 dB and 22 dB, respectively. Meanwhile, good selectivity below −15 dB from 2.7 GHz to 5.6 GHz is achieved. The fabricated band-pass filter possesses stop-band up to 30 GHz with a rejection greater than 17 dB and a compact size of 24 mm $*$ 14.7 mm. The measured frequency response is shown in Fig. 12. Table 1 gives comparison between this work and some recently reported dual-band filters. (f_0) in the table means the first passband of the dual-band filter. On the other hand, S_{11} is as small as −8 dB and −11 dB around 20 GHz and above 27 GHz respectively because of the SMA loss and the vector network analyzer error. However, the design with wide stop-band should be correct based on the simulated results in Fig. 10(c).

Table 1. Some references for dual-band filter comparison.

Ref.	Size	stopband (below −20 dB)	center frequency
1	about 10.2 mm * 12.3 mm (two resonators on one layer)	to 7 GHz ($2.9f_0$)	2.4 GHz/5.2 GHz
2	about 145 mm * 30 mm (resonators on one layer)	to 20 GHz ($8.3f_0$)	2.4 GHz/6 GHz
3	about 26 mm * 8 mm (two resonators on one layer)	to 7 GHz ($2.9f_0$)	2.4 GHz/5.7 GHz
4	about 33.1 mm * 27.7 mm (two resonators on one layer)	to 2.8 GHz ($1.6f_0$)	1.8 GHz/2.4 GHz
5	about 22.9 mm * 15 mm (two resonators on one layer)	to 9 GHz ($3.67f_0$)	2.45 GHz/5.7 GHz
6	about 46 mm * 15 mm (resonators on one layer)	to 10 GHz ($4f_0$)	2.5 GHz/8 GHz
7	about 55 mm * 30 mm (resonators on one layer)	to 5.8 GHz ($1.6f_0$)	3.65 GHz/5.2 GHz
8	about 75 mm * 30 mm (resonators on one layer)	to 7 GHz ($2f_0$)	3.5 GHz/5.2 GHz
9	about 30 mm * 27 mm (resonators on one layer)	to 8 GHz ($3.3f_0$)	2.4 GHz/3.6 GHz
10	about 75 mm * 26 mm (resonators on one layer)	to 18.5 GHz ($7.7f_0$)	2.4 GHz/5.8 GHz
11	about 55 mm * 26 mm (resonators on one layer)	to 4 GHz ($2.2f_0$)	1.8 GHz/2.75 GHz
12	about 25 mm * 40 mm (resonators on one layer)	to 4 GHz ($2.5f_0$)	1.6 GHz/3.4 GHz
13	about 30 mm * 52 mm (resonators on one layer)	to 11.8 GHz ($3.1f_0$)	3.7 GHz/5.8 GHz
14	about 27 mm * 53 mm (resonators on one layer)	to 4.8 GHz ($6f_0$)	0.8 GHz/1.6 GHz
This work	about 24 mm * 14.7 mm (two resonators on two different layers)	to 30 GHz ($12f_0$)	2.46 GHz/5.86 GHz

4. CONCLUSION

In this paper, a novel compact dual-band band-pass filter with the stop-band up to 30 GHz is proposed. Moreover, the size of this filter

can be also reduced by using two resonators at two layers connecting by via holes. The passbands locate at 2.43 GHz–2.52 GHz and 5.83 GHz–5.92 GHz. Furthermore, the good selectivity has been achieved that the stop-band below −15 dB between two passbands is from 2.7 GHz to 5.6 GHz. Meanwhile, the stop-band is up to 30 GHz. All of this good performance is reached in a compact size as small as 24 mm ∗ 14.7 mm.

REFERENCES

1. Sun, S. and L. Zhu, "Compact dual-band Micro-strip band-pass filter without external feeds," *IEEE Microw. Wireless Compon. Lett.*, Vol. 15, No. 10, 644–646, Oct. 2005.
2. Kuo, J.-T. and H.-P. Lin, "Dual-band band-pass filter with improved performance in extended upper rejection band," *IEEE Trans. on Microw. Theory and Tech.*, Vol. 57, No. 4, Apr. 2009.
3. Chen, C.-Y. and C.-Y. Hsu, "A simple and effective method for micro-strip dual-band filters design," *IEEE Microw. Wireless Compon. Lett.*, Vol. 16, No. 3, 246–248, May 2006.
4. Zhang, X. Y., J. Shi, J.-X. Chen. and Q. Xue, "Dual-band band-pass filter design using a novel feed scheme," *IEEE Microw. Wireless Compon. Lett.*, Vol. 19, No. 6, 350–352, Jun. 2009.
5. Chen, C.-Y., C.-Y. Hsu, and H.-R. Chuang, "Design of miniature planar dual-band filter using dual-feeding structures and embedded resonators," *IEEE Microw. Wireless Compon. Lett.*, Vol. 16, No. 12, 669–671, Dec. 2006.
6. Marimuthu, J., A. M. Abbosh, and B Henin, "Planar microstrip bandpass filter with wide dual bands using parallel-coupled lines and stepped impedance resonators," *Progress In Electromagnetics Research C*, Vol. 35, 49–61, 2013.
7. Wang, J., H. S. Ning, Q. X. Xiong, M. Q. Li, and L. F. Mao, "A novel miniaturized dual-band bandstop filter using dual-plane defected structure," *Progress In Electromagnetics Research*, Vol. 134, 397–417, 2013.
8. Chu, Q.-X. and Z.-H. Li, "High-order dual-band bandpass filter with independently controllable frequencies and bandwidth," *Progress In Electromagnetics Research C*, Vol. 30, 253–265, 2012.
9. Kuo, J.-T. and S.-W. Lai, "New dual-band bandpass filter with wide upper rejection band," *Progress In Electromagnetics Research*, Vol. 123, 371–384, 2012.
10. Mashhadi, M. and N. Komjani, "Design of dual-band band-pass filter with wide upper stopband using SIR and GSIR structures," *Progress In Electromagnetics Research C*, Vol. 32, 221–232, 2012.

11. Deng, K., S. Yang, S. J. Sun, B. Wu, and X. W. Shi, "Dual-mode dual-band bandpass filter based on square loop resonator," *Progress In Electromagnetics Research C*, Vol. 37. 119–130, 2013.
12. Sun, S. J., S. Yang, B. Wu, K. Deng, and C. H. Liang, "Dual-band bandpass filter using a single short-ended dual-mode resonator with adjustable first passband," *Progress In Electromagnetics Research C*, Vol. 37, 95–106, 2013.
13. Wu, Y.-L., C. Liao, and X.-Z. Xiong, "A dual-wideband bandpass filter based on e-shaped microstrip sir with improved upper-stopband performance," *Progress In Electromagnetics Research*, Vol. 108. 141–153, 2010.
14. Kuo, J.-T., C.-Y. Fan, and S.-C. Tang, "Dual-wideband bandpass filters with extended stopband based on coupled-line and coupled three-line resonators," *Progress In Electromagnetics Research*, Vol. 124, 1–15, 2012.
15. Luo, X. and J.-G. Ma, "Compact slot-line bandpass filter using backside microstrip open-stubs and air-bridge structure for spurious suppression," *APMC*, 882–885, 2009.
16. Xu, F., M. Xiao, Z. Wang, J. Cui, Z. Zhu, M. Ju, and J. Duan, "Compact bandpass filter with wide stopband using rectangular strips, asymmetric open-stubs and L slot lines," *Progress In Electromagnetics Research C*, Vol. 40, 201–215, 2013.